

**Achievement of high efficiency and thermally stable near-infrared phosphors by designing
chromium crystallographic environment for nondestructive testing and night vision**

Guohui Wei, Panlai Li*, Rui Li, Ye Wang, Hao Suo, Yuanbo Yang, Shaoxuan He, Jiehong Li,

Yawei Shi, Zhijun Wang*

Hebei Key Laboratory of Optic-electronic Information and Materials, College of Physics Science &
Technology, Hebei University, Baoding 071002, China

Table S1 Refined crystallographic data of $\text{InTaO}_4:\text{Cr}^{3+}$ ($x=0\text{-}0.011$).

*li_panlai@126.com

*wangzj1998@126.com

x	0	0.001	0.003	0.005	0.007	0.009	0.011
Crystal System	monoclinic-type						
Space group	P2/a						
a (Å)	5.1588	5.1575	5.1578	5.1582	5.1571	5.1575	5.1566
b (Å)	5.7792	5.7777	5.7779	5.7781	5.7769	5.7772	5.7761
c (Å)	4.8287	4.8274	4.8274	4.8276	4.8263	4.8265	4.8256
Z	4						
Cell Volume (Å³)	143.920	143.823	143.803	143.744	143.727	143.671	143.651
R _{wp} (%)	8.70	9.05	8.57	8.96	8.84	10.02	8.97
R _p (%)	6.79	7.12	6.02	6.99	6.98	7.75	7.00
χ^2	1.202	1.292	1.16	1.223	1.228	1.554	1.221

Table S2 Refined crystallographic data of ScTaO₄:Cr³⁺ (x=0- 0.011).

x	0	0.001	0.003	0.005	0.007	0.009	0.011
Crystal System	monoclinic-type						
Space group	P2/a						
a (Å)	5.1876	5.1575	5.1237	5.1145	5.1103	5.1073	5.1052
b (Å)	5.7781	5.7772	5.6802	5.6674	5.6635	5.6593	5.6572
c (Å)	4.8277	4.8265	4.8263	4.8072	4.8033	4.7995	4.7971
Z				4			
Cell Volume (Å³)	143.771	143.691	143.665	143.286	142.747	142.571	142.441
R _{wp} (%)	8.42	9.05	8.57	8.97	8.98	9.05	8.97
R _p (%)	7.92	7.85	7.86	7.99	7.68	7.75	7.78
χ^2	2.245	1.992	2.216	2.41	1.998	2.134	2.129

Table S3 Refined crystallographic data of GaTaO₄:Cr³⁺ (x=0- 0.011).

x	0	0.001	0.003	0.005	0.007	0.009	0.011
Crystal System	monoclinic-type						
Space group	P2/a						
a (Å)	4.5936	4.5934	4.5930	4.5928	4.5863	4.5828	4.5755
b (Å)	5.5717	5.5711	5.5710	5.5684	5.5664	5.5620	5.5598
c(Å)	4.9680	4.9666	4.9660	4.9631	4.9615	4.9588	4.9561

Z	4						
Cell Volume (Å ³)	127.150	127.099	127.067	127.007	126.990	126.702	126.607
R _{wp} (%)	9.95	9.65	8.69	8.43	8.54	8.02	8.97
R _p (%)	7.56	7.22	6.95	6.86	6.92	6.75	7.38
χ^2	2.505	2.794	2.265	2.443	2.678	2.362	2.267

Table S4 Content ratio of each element of GaTaO₄:Cr³⁺

Element	Atomic (%)
O	84.8
Ga	18.8
Ta	37.2
Cr	0.7

Table S5 Content ratio of each element of ScTaO₄:Cr³⁺

Element	Atomic (%)
O	64.4
Sc	23.2
Ta	51.9
Cr	1.1

Table S6 Content ratio of each element of InTaO₄:Cr³⁺

Element	Atomic (%)
O	54.1

In	21.9
Ta	22.3
Cr	1.7

Table S7. Calculation of the relative formation energy of GaTaO_4 and $\text{Ga}[\text{Ta}_{\text{Cr}}]\text{O}_4$.

Substituting model	GaTaO_4	$\text{GaTa}_{\text{Cr}}\text{O}_4$
Formation energy (eV)	-14.3671 eV	-8.6370 eV

Measurements of quantum efficiency

The quantum efficiency (QE) measurement was performed at room temperature by using a HORIBA FLUorolog3 fluorescence spectrometer with a 450 W Xe lamp. The IQE is defined as the percentage of the number of emitted photons to that of absorbed photons, which can be calculated using the following equation:

$$IQE = \frac{\int L}{\int E_R - \int E_S} \quad (1)$$

L is the luminescence spectrum of the sample, E_S is the excitation spectrum of the sample, and E_R is the excitation spectrum referenced by BaSO_4 . In addition, the EQE is defined as the percentage of the number of emitted photons to the number of exciting photons:

$$EQE = \frac{\int_L}{\int E_R} \times 100\% \quad (2)$$

The absorption efficiency (AE) is defined as the percentage of the number of absorbed photons (by the sample) to that of excitation photons:

$$AE = \frac{\int E_R - \int E_S}{\int E_R} \times 100\% \quad (3)$$

Measurements of Huang–Rhys factor (S)

$$FWHM = 2.36\sqrt{S}\hbar\omega\sqrt{\coth(\frac{\hbar\omega}{2kT})} \quad (4)$$

where the $FWHM$ (eV) is the full width at half maximum of emission spectrum at temperature T (K), and the $\hbar\omega$ and k are the phonon energy and Boltzmann's constant, respectively.

$$\coth(x) = \frac{e^x + e^{-x}}{e^x - e^{-x}} \quad (5)$$

$$FWHM^2 = 5.57 \times S \times (\hbar\omega)^2 \left(1 + \frac{1}{\frac{\hbar\omega}{kT} - 1}\right) \quad (6)$$

$$\frac{\hbar\omega}{kT} \approx 10^{-3} \quad (7)$$

$$FWHM^2 = 5.57 \times S \times (\hbar\omega)^2 \left(1 + \frac{1}{\frac{\hbar\omega}{2kT}}\right) \quad (8)$$

$$FWHM = a + b \times 2kT \quad (9)$$

$$a = 5.57 \times S \times (\hbar\omega)^2 \quad (10)$$

$$b = 5.57 \times S \times (\hbar\omega)^2 \quad (11)$$

Straight-line fitting equation:

$$\text{InTaO}_4: y = 0.36454x + 0.00454$$

$$\text{ScTaO}_4: y = 0.57179x + 0.01892$$

$$\text{GaTaO}_4: y = 0.39389x + 0.01987$$

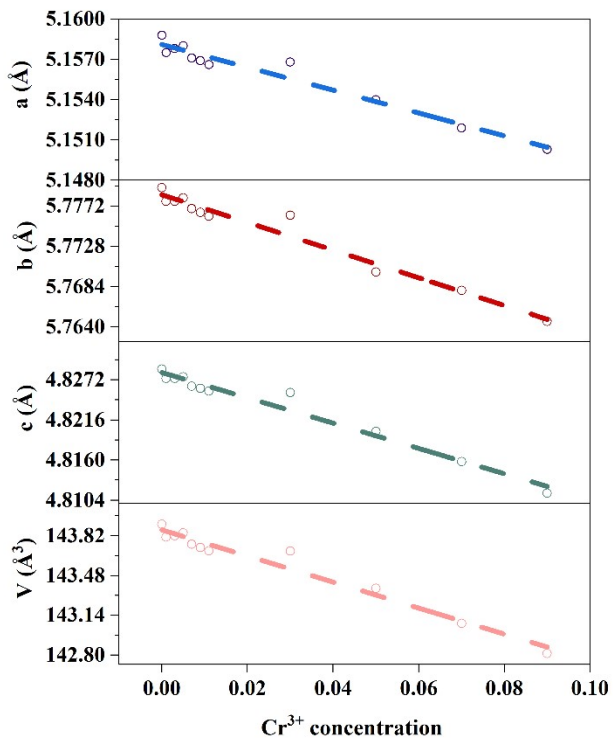


Figure S1 The trend of volume change of a, b, c, V of $\text{InTaO}_4: x\text{Cr}^{3+}$ ($x=0-0.1$).

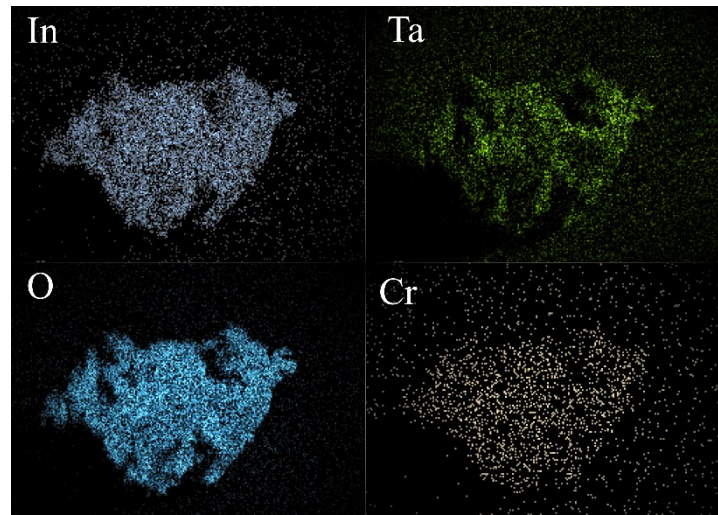


Figure S2 Mapping of InTaO₄:Cr³⁺.

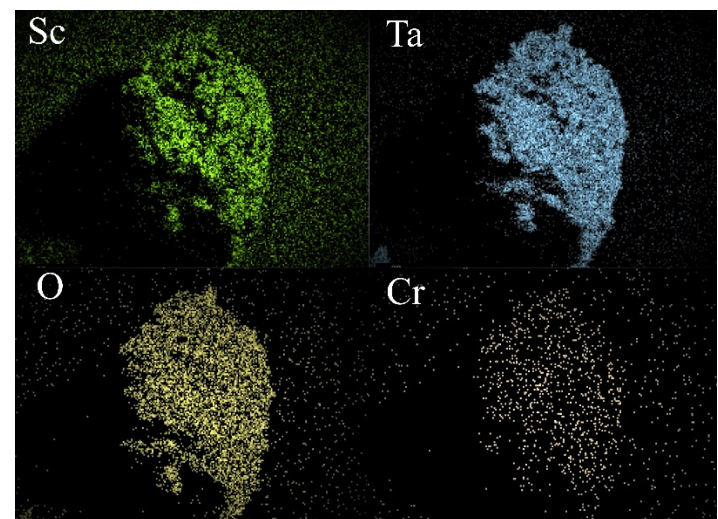


Figure S3 Mapping of ScTaO₄:Cr³⁺.

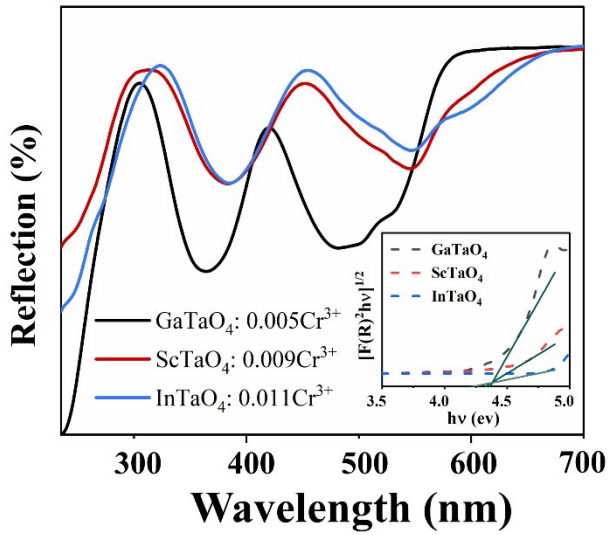


Figure S4 The diffuse reflectance spectra (DRs) of $\text{XTaO}_4:\text{Cr}^{3+}$ ($\text{X}=\text{Ga, Sc, In}$). The inset shows the XTaO_4 ($\text{X}=\text{Ga, Sc, In}$) host of linear relationship with $[\text{F}(\text{R})^2\text{hv}]^{1/2}$ and hv .

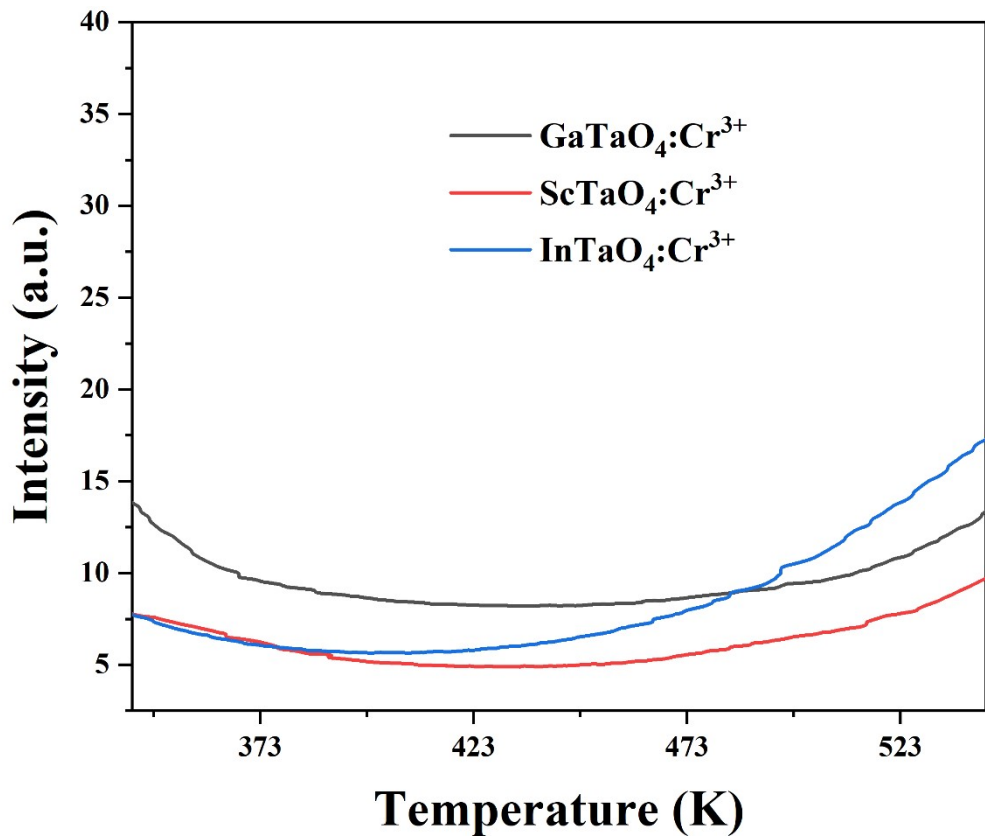


Figure S5 The thermoluminescence spectra of $\text{XTaO}_4:\text{Cr}^{3+}$ ($\text{X}=\text{Ga, Sc, and In}$).

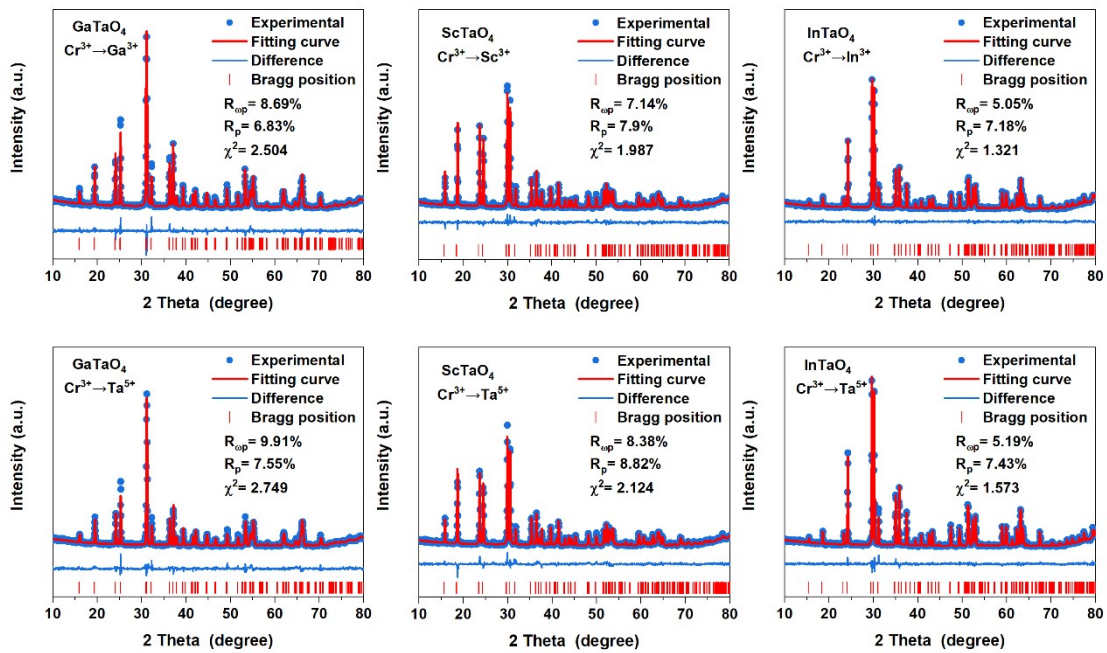


Figure S6 Rietveld refinement of XRD results of X^{3+} and Ta^{5+} ions are substituted by Cr^{3+} ions, respectively.

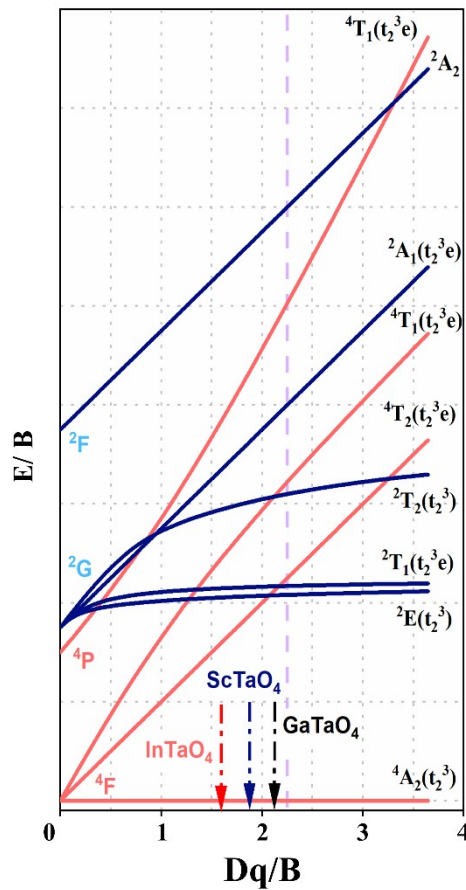


Figure S7 T–S diagram of Cr^{3+} at an octahedron crystal environment.

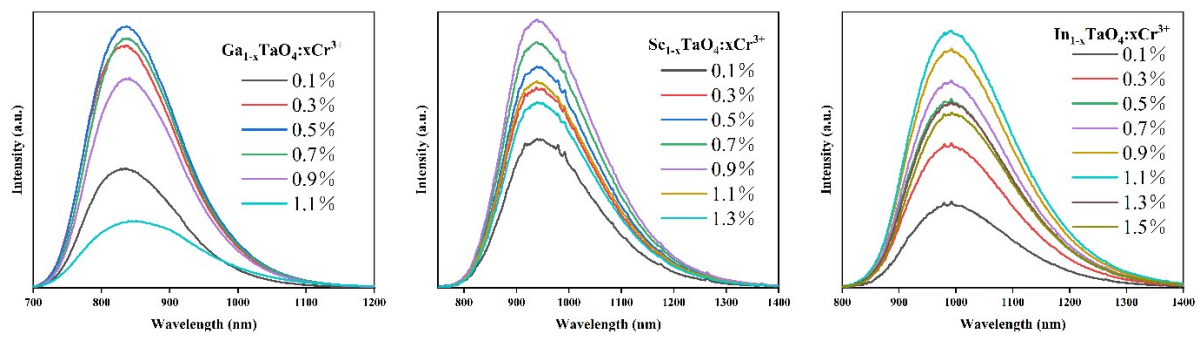


Figure S8 The PL spectrum of $\text{XTaO}_4:\text{Cr}^{3+}$ (X=Ga, Sc, In).

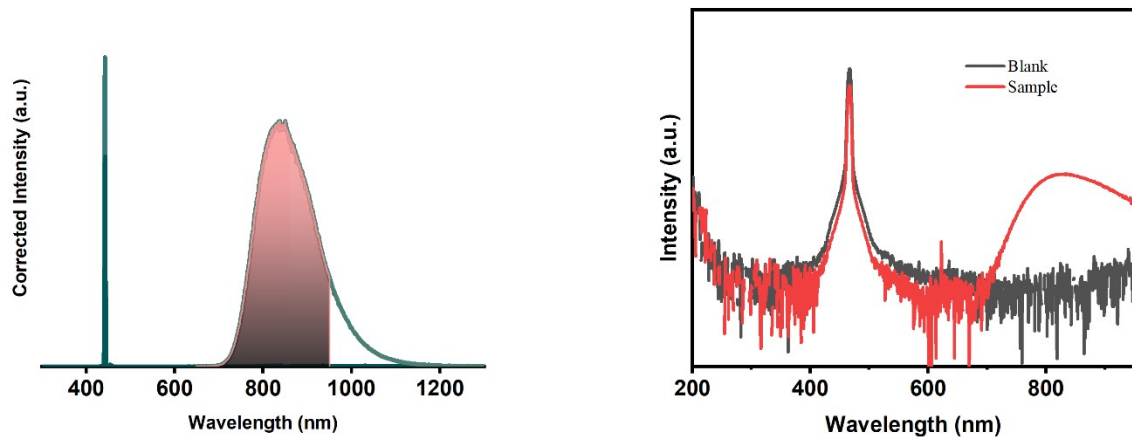


Figure S9 The luminescent spectra for the IQE of $\text{GaTaO}_4:0.005\text{Cr}^{3+}$.

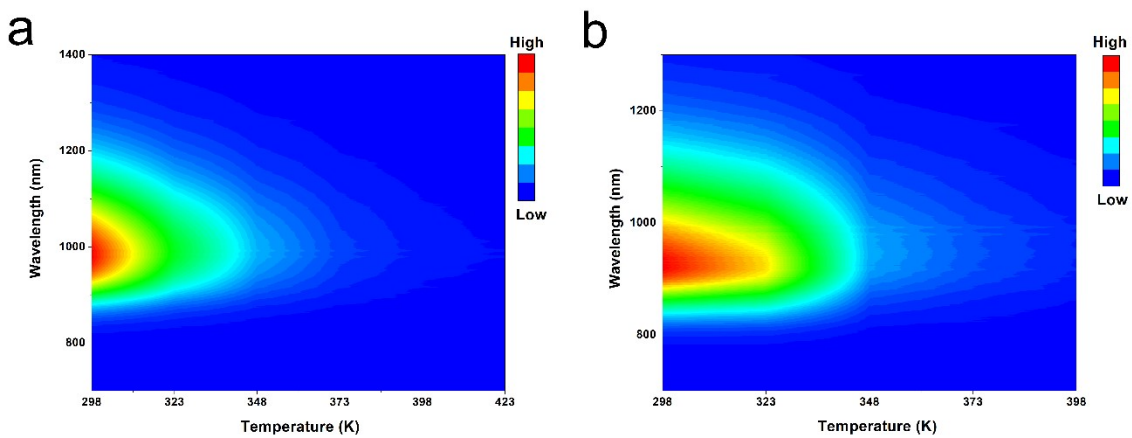


Figure S10 Temperature-dependent PL spectra of samples $\text{ScTaO}_4:0.009\text{Cr}^{3+}$ and $\text{InTaO}_4:0.011\text{Cr}^{3+}$.

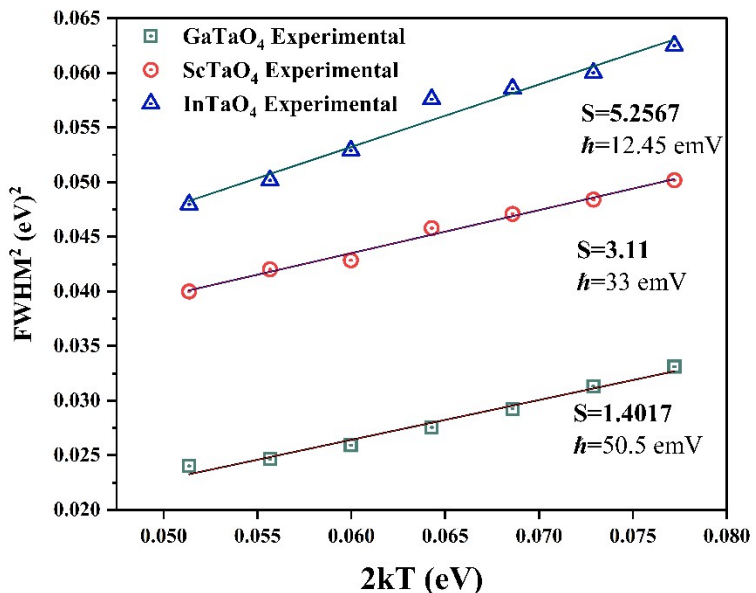


Figure S11 Fitting results of FWHM^2 as a function $2kT$.

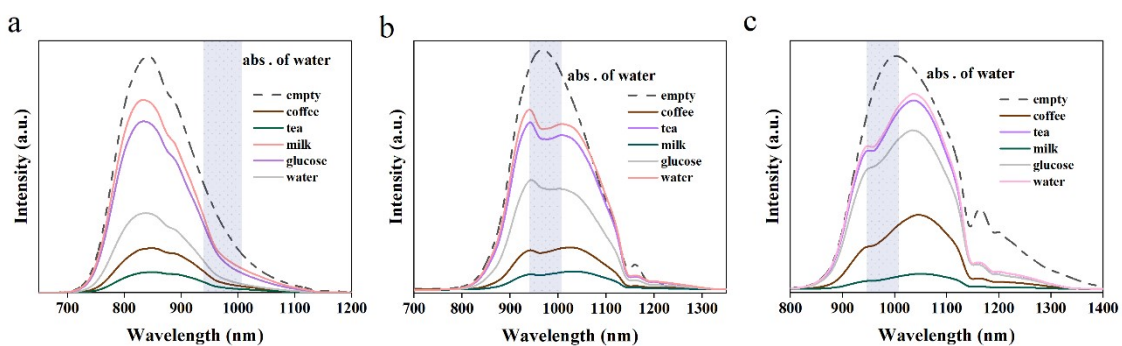


Figure S12 Spectra of LEDs coupled with XTaO₄: (X= Ga, Sc, and In) penetrating five different solutions respectively